Conference Proceedings

Solar World Congress 2015
Daegu, Korea, 08 – 12 November 2015

Uncertainty evaluation of measurements with pyranometers and pyrheliometers

Jörgen Konings[1] and Aron Habte[2]

1 Hukseflux Thermal Sensors B.V., Delft (the Netherlands)

2 National Renewable Energy Laboratory, Golden, CO (U.S.)

Abstract

Evaluating photovoltaic (PV) cells, modules, arrays and systems performance of solar energy relies on accurate measurement of the available solar radiation resources. Solar radiation resources are measured using radiometers such as pyranometers (global horizontal irradiance) and pyrheliometers (direct normal irradiance).

The accuracy of solar radiation data measured by radiometers depends not only on the specification of the instrument but also on a) the calibration procedure, b) the measurement conditions and maintenance, and c) the environmental conditions. Therefore, statements about the overall measurement uncertainty can only be made on an individual basis, taking all relevant factors into account. This paper provides guidelines and recommended procedures for estimating the uncertainty in measurements by radiometers using the Guide to the Expression of Uncertainty (GUM) Method.

Special attention is paid to the concept of data availability and its link to uncertainty evaluation.

Keywords: *uncertainty evaluation, pyranometer, pyrheliometer, measurement, data availability*

1. Introduction

Within the American Society for Testing and Materials (ASTM) International Subcommittee G03.09 on Radiometry, a standard is developed that provides guidance and best practices for evaluating uncertainties when calibrating and performing outdoor measurements with pyranometers and pyrheliometers. The standard will describe a procedure that follows the guidelines in the Guide to the Expression of Uncertainty in Measurement, the GUM (JCGM 100, 2008). This method has been successfully applied to uncertainty evaluations of calibrations of and measurements with pyranometers and pyrheliometers (Habte et al., 2014; Reda et al., 2008; Reda, 2011).

The use of the GUM has become an accepted method to perform uncertainty evaluation, and for example the Baseline Surface Radiation Network (BSRN) recommends that all uncertainty calculations follow the procedure of the guide (McArthur, 2005). Within BSRN, a working group on uncertainty is established with the goal to calculate the uncertainty of BSRN data.

To illustrate the individual steps in the process of uncertainty evaluation, and to clarify the choices made, we present a worked example using real world data. We selected one day of pyranometer data from the National Renewable Energy Laboratory (NREL) Baseline Measurement System, located in Golden, CO, U.S; the 8th of June 2015 (Andreas and Stoffel, 1981). We assume that the pyranometer used to take these measurements is a secondary standard pyranometer with specifications that exactly match the requirements of its category. State of the art pyranometers have specifications that exceed the requirements of the ISO secondary standard category, and can reach lower uncertainties than presented here.

We go through both the formulation stage and the calculation stage in detail. We analyse the relative importance of the different uncertainty contributions, and make the link between uncertainty evaluation and the concept of data availability. Data availability is a new concept, which will be defined in chapter 4.

doi:10.18086/swc.2015.07.15 Available at http://proceedings.ises.org

2. Formulation stage: development of measurement model

We define the output quantity, or measurand, E as the one-minute average of global horizontal irradiance in W m^{-2}.

In the most basic pyranometer measurement model, the irradiance depends on two input quantities only:

- V, the pyranometer voltage output, measured in V
- S, the sensitivity of the pyranometer in V W^{-1} m^2

The measurement model is straightforward

$$\mathrm{E} = \frac{\mathrm{V}}{\mathrm{S}} \qquad \text{(eq. 1)}$$

Other, more complicated, measurement models for pyranometers are in use that include corrections for systematic dependencies; i.e. temperature response, directional response, or response to net longwave radiation (zero off-set a). The process of uncertainty evaluation does not change, although the mathematics become more involved. For the scope of this paper, we limit ourselves to the basic measurement model.

With the measurement model established, the next step is to come up with factors that affect the uncertainty of the measurement. All factors are attributed to a specific quantity. The GUM only allows for uncertainty sources that apply to the input parameters. We present an approach where we also allow uncertainty sources to apply directly to the output parameter. The reasoning behind this is that certain pyranometer and pyrheliometer characteristics are stated explicitly in W m^{-2}, and are therefore best applied to the irradiance.

The GUM states that all knowledge of the (input) quantities is inferred from either repeated indication values (Type A evaluation of uncertainty) or scientific judgement (Type B evaluation of uncertainty). In high end meteorological networks such as the BSRN, it is considered best practice to take readings at a frequency of 1 Hz and store data as one-minute averages, together with the one-minute standard deviation, minimum and maximum value. However, irradiance is never constant; the 60 readings within a minute are not truly repeated observations. The variation within the minute can be caused by instrumental variation, but just as well by atmospheric variations on short timescales. Therefore, we argue that the standard deviation should not be taken into account when calculating the measurement uncertainty of a pyranometer or pyrheliometer measurement.

Without any Type A contributions present, all contributions are treated as Type B. For a Type B evaluation of uncertainty, often the only available information is that the quantity lies in a specified interval [a, b]. In these cases, the GUM recommends to use a rectangular or uniform probability distribution with limits a and b.

The judgement of which uncertainty sources to include or exclude has to be made on an individual basis for every application, and is fundamental to the process of uncertainty evaluation. We present a set of possible sources per uncertainty source, discuss the relevance, and assign specification limits.

3.1 Uncertainty contributions to the pyranometer voltage output

The voltage output of the pyranometer is measured with a device called a data logger: a voltmeter with the ability to store measurements. The manufacturer of the data logger normally specifies the measurement accuracy. In our scenario, we use a data logger with a specified accuracy of 10 µV, and treat this accuracy as a symmetric specification limit.

3.2 Uncertainty contributions to the sensitivity of the pyranometer

For the sensitivity S, we use the value as given by the manufacturer as 15.00 µV W^{-1} m^2 ± 0.15 µV W^{-1} m^2 where the number following the ± symbol is the expanded uncertainty with a coverage factor k = 2.

Calibration reference conditions are given as 20 °C instrument temperature, normal incidence solar radiation, horizontal mounting and an irradiance level of 500 W m^{-2}. This calibration is a single point calibration, which is different from the traditional meteorological calibration which results in an average sensitivity valid for a range of temperatures, angles of incidence and irradiance levels.

The term 'reference conditions' should be understood as the operating conditions under which the specified instrumental measurement uncertainty is the smallest possible (JCGM 200, 2012). In the theoretical case where all measurements would take place under these reference conditions, the calibration uncertainty as given by the manufacturer would suffice as the only contribution to the input quantity *S*. In practice, because all data points deviate from the reference conditions, the instrument characteristics have to be included in the uncertainty budget as well.

The most common set of characteristics is the list defined in ISO 9060 (ISO 9060, 1990) and most pyranometer and pyrheliometer manufacturers specify their instruments accordingly. These characteristics are defined both for pyranometers and pyrheliometers.

Of that list, the following apply to the input quantity sensitivity *S*.

- non-stability, the percentage change in sensitivity per year, relevant if the instrument has not been recalibrated recently. For our pyranometer, the secondary standard specification limit of 0.8 % per year applies. As the most recent calibration is about one year ago, we will use 0.8 % as a specification limit. ISO 9060 lists non-stability as a symmetric source, but we treat this uncertainty source as one-sided: the most common source of non-stability in thermal pyranometers is degradation of the black coating that absorbs the solar radiation. The coating can become less black over time, leading to a reduction in sensitivity. We use specification limits of [-0.8 %, 0 %].
- non-linearity, the change in sensitivity of the instrument for irradiance levels other than the reference condition (500 W m^{-2}) between 100 and 1000 W m^{-2}. We use the secondary standard specification limit of ± 0.5 % and apply it to the full measurement range.
- temperature response, the change in sensitivity of the instrument for temperatures other than the reference condition (20 °C). ISO 9060 states a limit of 2 % percentage deviation due to change in ambient temperature within an interval of 50 °C. In our scenario, the range of ambient temperatures is smaller than 50 °C, but we will use a specification limit of ± 1 % as a conservative estimate.
- tilt response, the change in sensitivity of the instrument for mounting orientations other than the reference condition (horizontal). In our example, we do not include the tilt response characteristic, because we are measuring global horizontal irradiance. When we measure tilted solar radiation with a pyranometer (for example in a plane-of-array setup) or direct solar radiation with a pyrheliometer, we do have to include tilt response in the uncertainty budget.

The ISO 9060 list of characteristics is not exhaustive; other effects can be considered as well. For our scenario, we will include an uncertainty contribution related to the level of maintenance. Pyranometer domes are subject to fouling. Fouling can be a continuous process, a slowly building layer of dust, or appear in bursts, for example due to sandstorms. The severity depends on the local conditions. For our scenario, clean air and daily cleaning, we estimate a maximum contribution of 0.5 %. This estimate is not based on any documented numbers, but is based on experience with and general knowledge of the behaviour of the instrument. In the GUM framework, this is allowed under the general header of 'scientific judgement'.

3.3 Uncertainty contributions to the global horizontal irradiance

We include three uncertainty sources that apply directly to the output quantity, the irradiance

- zero off-set a, the response to net thermal radiation. The pyranometer domes exchange radiation with the cold clear sky, cooling them down. This results in a negative offset in the irradiance. ISO 9060 specifies a limit of 7 W m^{-2} for 200 W m^{-2} thermal exchange. The thermal exchange, or net longwave radiation, varies with atmospheric conditions and altitude. 200 W m^{-2} is typical for very clear sky conditions at altitude, which fits nicely for our scenario. The offset is negative only, we use specification limits of [-7 W m^{-2}, 0 W m^{-2}]
- zero off-set b, the response to temperature gradients. As the ambient temperature increases and decreases, different parts of the instrument can be out of thermal equilibrium. ISO 9060 specifies a maximum value off-set of ± 2 W m^{-2} for a gradient of 5 °C per hour. We will use this value.
- directional response, the error caused by assuming the sensitivity to a normal incidence beam of irradiance is valid when measuring beams coming from any direction. ISO 9060 uses a specification limit of 10 W m^{-2} for a beam whose normal irradiance is 1000 W m^{-2}. In practice, this means that the relative specification limit is different with the position of the sun in the sky. With the sun in zenith (normal

incidence) the 10 W m^{-2} error on the normal incidence beam of 1000 W m^{-2} leads to a specification limit of 10 W m^{-2}/1000 W m^{-2} = 1 %. With the sun at 60 ° from zenith, the same normal incidence beam of 1000 W m^{-2} contributes cos(60 °)·1000 W m^{-2} = 500 W m^{-2}. The specification limit due to the 10 W m^{-2} error is then 10 W m^{-2}/500 W m^{-2} = 2 %.

In our example, we have a separate measurement of direct irradiance E_{direct} available, so we can apply the error to the direct component of the global horizontal irradiance only

$$a = \frac{10\ \mathrm{W\ m^{-2}}}{E_{\mathrm{direct}} \cos \Theta z} \qquad \text{(eq. 2)}$$

with Θ_z the zenith angle.

When no separate measurement of direct irradiance is available, a decent estimate of the specification limit of the directional response can be found by replacing E_{direct} in equation 2 by the global horizontal irradiance E itself.

The uncertainty sources are summarized in table 1.

Tab. 1: Summary of uncertainty contributions

Uncertainty source	Parameter	Specification limit a	Type	Distribution	Shape
data logger accuracy	V	10 µV	B	rectangular	symmetric
calibration uncertainty	S	1.5 %	B	normal (k = 2)	symmetric
non-stability	S	0.8 %	B	rectangular	one-sided (negative)
non-linearity	S	0.5 %	B	rectangular	symmetric
temperature response	S	1 %	B	rectangular	symmetric
maintenance	S	0.5 %	B	rectangular	symmetric
zero off-set a	E	7 W m^{-2}	B	rectangular	one-sided (negative)
zero off-set b	E	2 W m^{-2}	B	rectangular	symmetric
directional response	E	$\frac{10\ \mathrm{W\ m^{-2}}}{E_{\mathrm{direct}} \cos \Theta z}$	B	rectangular	symmetric

With the measurement mode developed and all quantities characterized, the measurand E is fully specified in terms of this information. The rest is applying the algorithms as laid out in the GUM, but involves no further judgement or decisions.

3. Calculation stage: propagation of distributions and summary of expanded uncertainty

The GUM uncertainty framework uses the values of the input quantities, their standard uncertainties and the sensitivity coefficients to form an estimate of the output quantity and the associated combined standard uncertainty.

The standard uncertainty of a quantity is the square root of the sum of the squares of all uncertainty sources that apply to that parameter

$$u(X) = \sum_j u_j \qquad \text{(eq. 3)}$$

where j sums over all uncertainty sources that apply to the input quantity X.

The introduction of one-sided uncertainty sources should lead to asymmetric uncertainty distribution of the measurement. Our current method is not yet suited to handle this. We choose to halve the one-sided specification limits and treat them as symmetric. Future work should aim to improve on this, and allow asymmetric uncertainty distributions of the measurements.

We do not consider correlations between uncertainty sources in this method. Some uncertainty sources are clearly uncorrelated, such as data logger accuracy and non-stability, but others certainly have some level of correlation. Correlations, including correlations over time scales, are the subject of current research.

In table 2, the standard uncertainty of all quantities is calculated for the single data point at 11:45, with a pyranometer voltage output V of 15384 µV and a solar zenith angle Θ_z of 17.2°.

Tab. 2: Calculation of standard uncertainty of voltage output, sensitivity and irradiance for one data point

(Input) Quantity	Uncertainty source	u_i	Standard uncertainty
V = 15384 µV			
	data logger accuracy	10 µV	
			$u(V)$ = 10 µV
S = 15.00 µV W^{-1} m²			
	calibration uncertainty	0.08 µV W^{-1} m²	
	non-stability	0.03 µV W^{-1} m²	
	non-linearity	0.04 µV W^{-1} m²	
	temperature response	0.09 µV W^{-1} m²	
	maintenance	0.04 µV W^{-1} m²	
			$u(S)$ = 0.13 µV W^{-1} m²
E = 1025.6 W m^{-2}			
	zero off-set a	2.02 W m^{-2}	
	zero off-set b	1.15 W m^{-2}	
	directional response	5.92 W m^{-2}	
			$u(E)$ = 6.36 W m^{-2}

Note that the standard uncertainty of the irradiance u(E) is not the final result. The standard uncertainties in table 2 have to be combined to reach the so-called ‘combined standard uncertainty’ of the measurand $u_c(E)$. This is done using the law of propagation of uncertainty.

$$u_c(E) = \sqrt{c_V^2 u^2(V) + c_S^2 u^2(S) + c_E^2 u^2(E)} \qquad \text{(eq. 4)}$$

where c_V, c_S, c_E are the ‘sensitivity coefficients’ of quantities V, S and E respectively.

The sensitivity coefficient of a quantity is the partial derivative of the output quantity with respect to that quantity. GUM defines this only for input quantities, but the definition can be extended to the output quantity to give a sensitivity coefficient equal to one (eq. 7). For our measurement model, the sensitivity coefficients are

$$c_V = \frac{\partial E}{\partial V} = \frac{1}{S} \qquad \text{(eq. 5)}$$

$$c_S = \frac{\partial E}{\partial S} = -\frac{V}{S^2} \qquad \text{(eq. 6)}$$

$$c_E = \frac{\partial E}{\partial E} = 1 \qquad \text{(eq. 7)}$$

For the single data point we used as an example above, the combined standard uncertainty of the irradiance becomes

$$c_V = \frac{\partial E}{\partial V} = \frac{1}{S} = 0.07\ \mu\text{V}^{-1}\text{Wm}^{-2} \qquad \text{(eq. 8)}$$

$$c_S = \frac{\partial E}{\partial S} = -\frac{V}{S^2} = -68.37\ \mu V^{-1} W^2 m^{-4}$$ (eq. 9)

$$c_E = 1$$ (eq. 10)

$$u_c(E) = \sqrt{c_V^2 u^2(V) + c_S^2 u^2(S) + c_E^2 u^2(E)} = 11.2\ \mathrm{Wm}^{-2}$$ (eq. 11)

The combined standard uncertainty can be universally used to express the uncertainty of a measurement result, but it is preferable to define an interval about the measurement result that is expected to encompass a certain fraction of reasonable results for the measurand. This is achieved by multiplying the combined standard uncertainty with a coverage factor k to find the expanded uncertainty U. In practice, the coverage factor is chosen to reach a level of confidence of 95 %. The expanded uncertainty is then written with a subscript 95 to reflect this.

$$U_{95} = k u_c$$ (eq. 12)

This approach has the advantage of taking the abstract concept of uncertainty and applying a physical meaning. An irradiance reading of 1000 W m^{-2} with a symmetric expanded uncertainty U_{95} of 10 W m^{-2} can be understood to mean that if you would repeat that measurement 100 times, 95 times you would get a reading between 990 and 1010 W m^{-2}. This is a useful way of thinking when performing a risk analysis based on irradiance readings.

Choosing the right coverage factor is a complicated procedure, and is detailed in Annex G of the GUM (JCGM 100:2008). A simple approach is often adequate in measurement situations where the probability distribution is approximately normal and there is a significant number of effective degrees of freedom. When this is the case, one can use $k = 2$ to produce an interval having a level of confidence of 95 %, and $k = 3$ to produce an interval having a level of confidence of 99 %.

We introduced uncertainty sources with a rectangular probability distribution and although the effective degrees of freedom is significant (with a measurement rate of 1 Hz, we have 60 readings in the one-minute average), it is not infinite. However, we argue that using a coverage factor of 2 is a conservative and simple approach when analysing pyranometer of pyrheliometer measurements.

For the single data point, the final result is

$$U_{95}(E) = 2u_c(E) = 22.4\ \mathrm{Wm}^{-2}$$ (eq. 13)

The GUM recommends to report this measurement result as follows

"E = (1025.6 ± 22.4) W m^{-2}, where the number following the ± symbol is the numerical value of $U = ku_c$, with U determined from u_c = 11.2 W m^{-2} and k = 2 based on the normal distribution, and defines and interval estimated to have a level of confidence of 95 percent."

This result is valid for a single data point, but the analysis can be repeated for every data point. In this example, the only parameter that changes is the voltage output V, and therefore also the magnitude of the measurand E. When you perform this analysis over a full day, it can be seen that the expanded uncertainty varies over time.

In figure 1 the global horizontal irradiance is plotted with the expanded uncertainty drawn as error bars. As the irradiance increases, the absolute value of the expanded uncertainty increases as well, even as the relative value of the expanded uncertainty decreases.

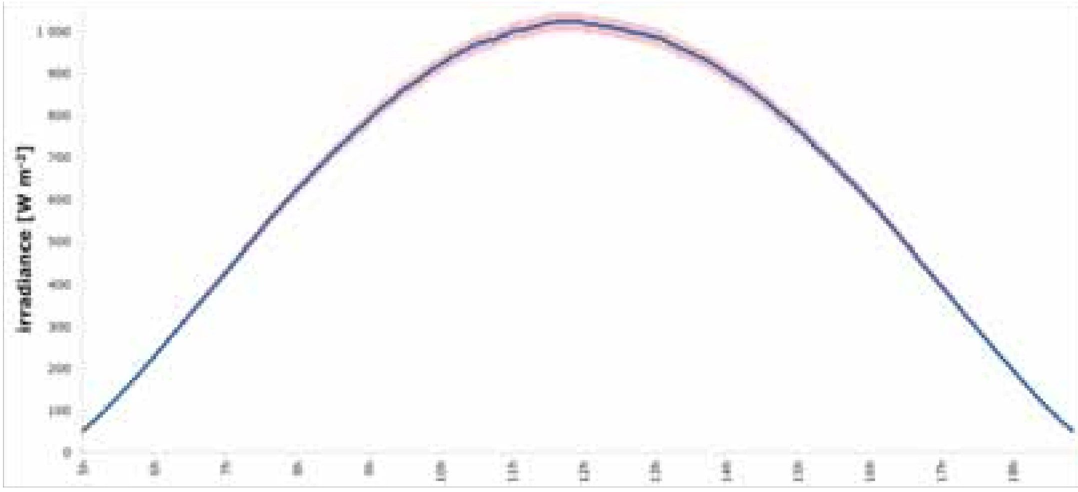

Fig. 1: Measured global horizontal irradiance as a function of time, red bars give the expanded uncertainty values that correspond with a level of confidence of 95 %.

4.1 Analysis of relative importance per uncertainty source

It is possible to calculate the relative contribution of each uncertainty source to the expanded uncertainty. This way, it is possible to judge which uncertainty sources are dominant for this application. This information can be useful for purchasing decisions, product development and/or help to decide which systematic errors should be corrected for.

To calculate the relative contribution of an uncertainty source, first calculate the relative importance of all quantities as the ratio of the standard uncertainty of the quantity to the sum of the standard uncertainty of all quantities, weighed by their sensitivity coefficients.

For a quantity *X* this is

$$\frac{u(X)}{\sum_l c_l u(l)} \qquad \text{(eq. 14)}$$

where *l* sums over all quantities

The relative importance of one uncertainty source within a quantity is found directly from the ratio of the standard uncertainty to the sum of the standard uncertainties of all sources that apply to that specific quantity.

For an uncertainty source *i* this is

$$\frac{u_i}{\sum_m u_m} \qquad \text{(eq. 15)}$$

where *m* sums over all uncertainty sources that apply to the same quantity as *i*.

Multiply the two ratios to find the final contribution.

We work this out for three sources explicitly, and present the contributions of all sources in table 3, for the same single data point.

$$\frac{u_{\text{data logger accuracy}}}{\sum_{i=\text{data logger accuracy}} u_i} \cdot \frac{u(V)}{c_V u(V) + c_S u(S) + c_E u(E)} = 4.1\ \% \qquad \text{(eq. 16)}$$

$$\frac{u_{\text{non-linearity}}}{\sum_{i=\text{calibration uncertainty, non-stability, non-linearity, temperature response, maintenance}} u_i} \cdot \frac{u(S)}{c_V u(V) + c_S u(S) + c_E u(E)} = 8.7\ \% \qquad \text{(eq. 17)}$$

$$\frac{u_{\text{zero off-set b}}}{\sum_{i=\text{zero off-set a, zero off-set b, directional response}} u_i} \cdot \frac{u(E)}{c_V u(V) + c_S u(S) + c_E u(E)} = 5.0\ \% \qquad \text{(eq. 18)}$$

Tab.3: Calculation of relative contribution to the expanded uncertainty per uncertainty source for one data point

Input quantity	Uncertainty source	Relative importance per input parameter	Relative importance per uncertainty source
V = 15384 µV			
	data logger accuracy		4.1 %
		4.1 %	
S = 15.00 µV W^{-1} m²			
	calibration uncertainty		15.0 %
	non-stability		6.9 %
	non-linearity		8.7 %
	temperature response		17.4 %
	maintenance		8.7 %
		56.7 %	
E = 1025.6 W m^{-2}			
	zero off-set a		8.7 %
	zero off-set b		5.0 %
	directional response		25.5 %
		39.2 %	

This procedure can be repeated for all data points. In figure 2, the expanded uncertainty is plotted as function of time, split per uncertainty source in a stacked area chart. Figure 2 a) gives the expanded uncertainty in W m^{-2}, figure 2 b) in percentage. For low irradiances, the uncertainty expressed in percentages becomes very high.

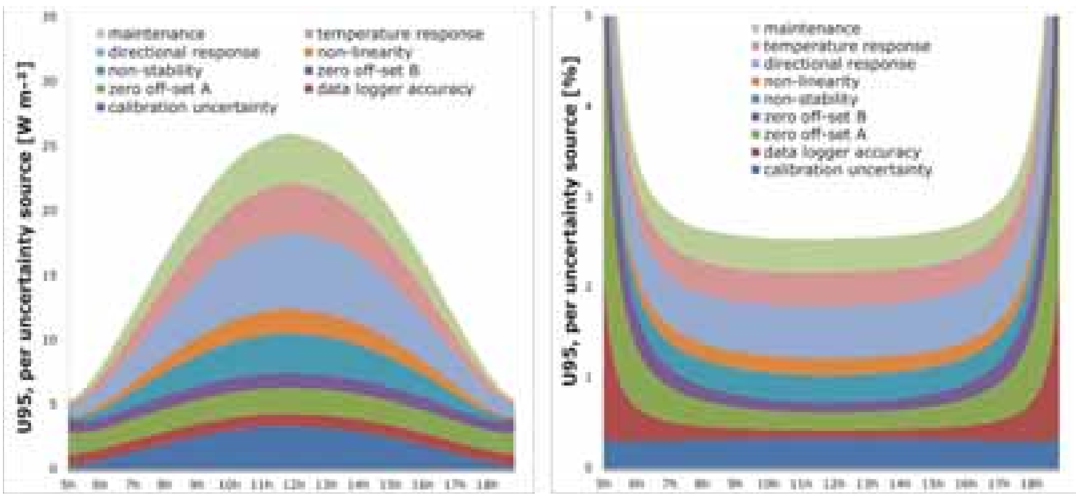

Fig. 2: Expanded uncertainty as function of time, split per uncertainty source.
The expanded uncertainty is expressed in a) absolute values in W m^{-2}, b) relative values in %.

In figure 3 we plot the relative contribution of each uncertainty source as a function of irradiance. Here it becomes clear that at low irradiance levels, the zero off-set a, dominates together with the zero off-set b and data logger accuracy. At higher irradiance levels, the directional response dominates, and the importance of the zero off-sets and data logger accuracy diminishes.

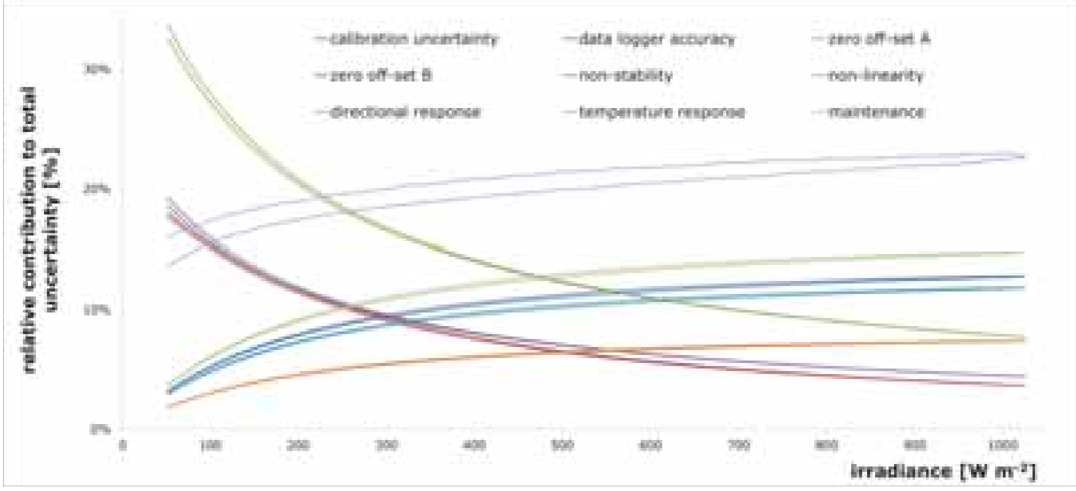

Fig. 3: Relative importance of each uncertainty source as a function of irradiance.

4. Data availability

The ‘rated operating conditions’ are defined as conditions that must be fulfilled during measurement in order that a measuring instrument performs as designed (JCGM 200:2012). For pyranometers and pyrheliometers, the condition that the optics (domes, windows) of the instrument are clean is a critical rated operating condition. Snowfall can obstruct the domes to no longer transmit solar radiation, leading to an underestimation. Rain droplets on a pyranometer can focus the incoming solar radiation, leading to an overestimation. Figure 4 gives visual examples of situations where the optics of the instrument are not clean.

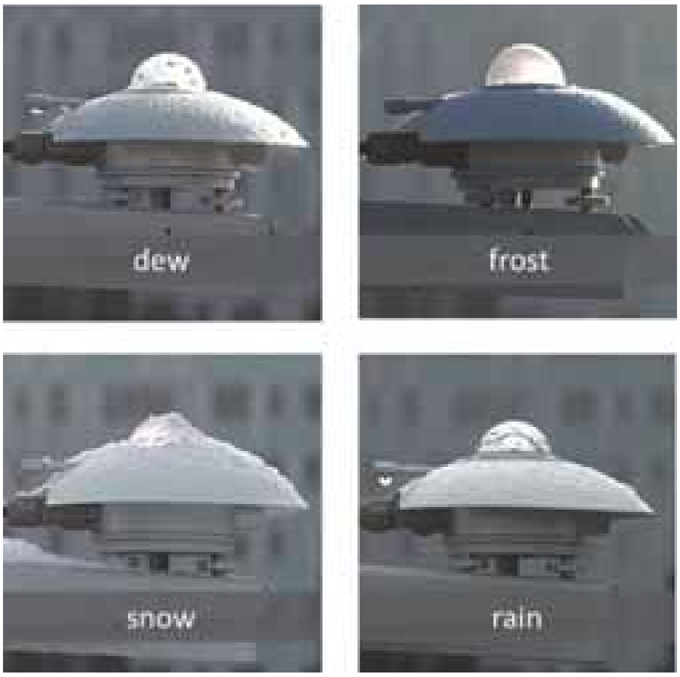

Fig. 4: Examples of pyranometers with domes that are not clean. These measurements cannot be assigned a meaningful measurement uncertainty.

In these situations, it is not possible to assign a meaningful measurement uncertainty to the instrument reading. Data points that fall outside the rated operating conditions should be flagged accordingly and considered as not available. This provides a definition of the concept of ‘data availability’: the percentage of data points over a certain time period that fall within the rated operating conditions of the instrument, and can be assigned a meaningful measurement uncertainty.

Data availability can be used as a requirement during site assessment, and can be useful for purchasing decisions or when determining the required level of maintenance during operation.

A trained user can recognize 'false' data point from a visual interpretation of the measurement data, but other methods are available that provide a more solid process of flagging data points. The BSRN uses a set of recommended Quality Control tests that compare measurement data with physically possible limits and extremely rare limits (Long 2012). A strong method is to combine separate measurements of global, diffuse and direct irradiance and compare the ratios between measured direct irradiance and the direct irradiance back-calculated from measurements of global and diffuse irradiance.

$$E_{\text{direct}} = E_{\text{global}} \cos \Theta z + E_{\text{diffuse}} \qquad \text{(eq. 19)}$$

When measurements of direct radiation are not available, which is often the case in solar energy applications, it can be helpful to monitor the pyranometers, for example using webcam images. A study using webcam images in Delft, the Netherlands, over 26 days in the spring of 2015, found that without any measures to improve data availability, an average 80 minutes of data per day was lost due to early morning dew.

Ways to improve the data availability of pyranometers and pyrheliometers include the use of forced ventilation (using purpose built ventilation units) and direct heating of the instrument optics to keep the optics above dew point temperature and free of frost and snow. Both methods can be effective, and in the study above were able to increase data availability to 100 %. Figure 5 shows the visual difference between a heated and unheated pyranometer during frost.

Fig. 5: Visual difference between a heated (left) and unheated (right) pyranometer during frost. Data points measured with the left pyranometer can be assigned a meaningful uncertainty, data points measured with the right pyranometer have to flagged as not available.

Both methods can also induce off-sets on the thermal instruments. These off-sets will have to be included as an uncertainty source, and can become dominant for instruments that were not designed for use with ventilation or heating. Especially in environments with extreme conditions, the user will have to find a balance between data availability and measurement uncertainty.

Instruments that are specifically designed for use with ventilation or direct heating in mind will often include ventilation or heating off-sets in the data sheet.

For example, the left pyranometer in figure 5 uses a combination of a sapphire outer dome with 1.5 W internal heating and specifies a heating off-set of 0 to -1.5 W m^{-2} (Hukseflux 2015). This uncertainty source should be applied directly to the irradiance, with a specification limit of 1.5 W m^{-2} and be treated as a Type B uncertainty with a one-sided (negative) rectangular distribution.

5. Results and discussion

We presented a worked example of the uncertainty evaluation of one clear sky day of global horizontal irradiance measured with a pyranometer specified as a secondary standard pyranometer.

We used a method based on the GUM, according to the procedures and guidelines that are written into a standard that is in development within the ASTM International Subcommittee G03.09 on Radiometry. In the formulation stage, we developed the measurement model and defined the relevant sources of uncertainty. In the calculation stage, we combined this information to find the expanded uncertainty of the measurement. As a separate analysis, we calculated the relative importance per uncertainty source.

We find an expanded uncertainty U95 of 2.2 % (k = 2) for a data point around solar noon, and we find the three dominant contributions to the measurement uncertainty; the directional response, the temperature response and the initial calibration uncertainty. For conditions with lower levels of irradiance, the zero off-sets and data logger accuracy become dominant.

Users have to adapt the analysis shown here to their own situation. In practice, this means they have to update the formulation stage with sources and specification limits for their own situation. The calculation stage does not change. Spreadsheets are available from the authors on request that can assist in this process.

The procedure presented is not capable of producing asymmetric confidence intervals, and does not incorporate correlations between different uncertainty sources, or correlations over time. Future work should improve on these matters.

We introduced the concept of data availability, and made a specific link of this concept with the process of uncertainty evaluation. Data availability can be a useful tool for site assessment, determining a maintenance schedule, purchasing decisions or product development.

6. References

Andreas, A., Stoffel, T., (1981). NREL Solar Radiation Research Laboratory (SRRL): Baseline Measurement System (BMS), Golden, Colorado (Data), NREL Report No. DA-5500-56488.

ISO 9060:1990(E) Solar energy - Specification and classification of instruments for measuring hemispherical solar and direct solar radiation.

JCGM 100:2008 Evaluation of measurement data – Guide to the expression of uncertainty in measurement (GUM).

JCGM 200:2012 International Vocabulary of Metrology – Basic and General Concepts and Associated Terms (VIM 3rd edition).

McArthur, L., 2005. World Climate Research Programme – Baseline Surface Radiation Network (BSRN) – Operations Manual Version 2.1.

Habte, A., Sengupta, M., Reda, I., Andreas, A., Konings, J., 2014. Calibration and Measurement Uncertainty Estimation of Radiometric Data: Preprint. 9 pp., NREL Report No. CP-5D00-62214.

Hukseflux, 2015, SR25_manual_v1508, User Manual SR25 Secondary standard pyranometer with sapphire outer dome, available from http://hukseflux.com/sites/default/files/product_manual/SR25_manual_v1508.pdf

Long, N., Dutton, E. G., 2012, BSRN Global Network recommended QC tests, V2.0, available from http://www.bsrn.awi.de/fileadmin/user_upload/redakteur/Publications/BSRN_recommended_QC_tests_V2.pdf

Reda, I.M., Myers, D.R., Stoffel, T.L., 2008. Uncertainty Estimate for the Outdoor Calibration of Solar Pyranometers: A Metrologist Perspective. NCSLI Measure, The Journal of Measurement Science, pp. 58-66.

Reda, I., 2011. Method to Calculate Uncertainty Estimate of Measuring Shortwave Solar Irradiance using Thermopile and Semiconductor Solar Radiometers. 20 pp., NREL Report No. TP-3B10-52194.